ELSEVIER

Ultramicroscopy 71 (1998) 149–157

ultramicroscopy

Tuning fork shear-force feedback

A.G.T. Ruiter*, K.O. van der Werf, J.A. Veerman, M.F. Garcia-Parajo, W.H.J. Rensen, N.F. van Hulst

Department of Applied Physics, Applied Optics Group & MESA Research Institute, University of Twente, P.O. Box 217, 7500 AE Enschede, The Netherlands

Abstract

Investigations have been performed on the dynamics of a distance regulation system based on an oscillating probe at resonance. This was examined at a tuning fork shear-force feedback system, which is used as a distance control mechanism in near-field scanning optical microscopy. In this form of microscopy, a tapered optical fiber is attached to the tuning fork and scanned over the sample surface to be imaged. Experiments were performed measuring both amplitude and phase of the oscillation of the tuning fork as a function of driving frequency and tip–sample distance. These experiments reveal that the resonance frequency of the tuning fork changes upon approaching the sample. Both the amplitude and the phase of the tuning fork can be used as distance control parameter in the feedback system. Using the amplitude a second-order behavior is observed, while with phase only a first-order behavior is observed. Numerical calculations confirm these observations. This first-order behavior results in an improved stability of the feedback system. As an example, a sample consisting of DNA strands on mica was imaged which showed the height of the DNA as 1.4 ± 0.2 nm.

1. Introduction

The probe in a near-field scanning optical microscope should be kept close to the sample surface. In practice, the probe to sample distance is kept below 10 nm. The most common technique to control this distance is based on the shear-force distance control mechanism, almost simultaneously implemented by Betzig [1] and Toledo-crow [2]. In this technique, the fiber is fixed to a vibrating element with a short part of the fiber (0.5–5 mm) extending from the vibrating element. This part is vibrated at resonance, pointing down towards the sample. Upon approaching the sample, a decrease in the amplitude of the oscillation is observed, generally attributed to a damping of the oscillation by the sample.

Detection of the oscillation amplitude of the fiber probe has been implemented using different methods. In one of the first experiments, Betzig [1] used a diffraction technique to measure the vibration amplitude of the fiber. A laser spot, diffracted by the fiber probe, was imaged onto a split detector generating a difference signal proportional to the oscillation amplitude. Also interferometric techniques have been implemented to measure the amplitude, using either a two-beam interferometer [2] or a fiber interferometer [3]. These techniques have

* Corresponding author. Tel.: + 31 53 4 894002; fax: + 31 53 4 891105; e-mail: a.g.t.ruiter@tnu.twente.nl.

0304-3991/98/$19.00
PII S0304-3991(97)00111-3

the disadvantage that additional stray light is brought into the vicinity of the aperture, disturbing the measurement of the near-field optical signal; moreover, accurate alignment of the external optics with respect to the probe is necessary. An alternative method is to use piezoelectric materials which generate a piezoelectric voltage proportional to the amplitude of the oscillation [4–7]. Based on this idea, the use of crystalline quartz tuning forks for detecting the probe's amplitude was demonstrated recently by Karraï [4]. In this case, the end of the fiber is attached to one arm of the fork and the tuning fork is oscillated at resonance, usually 33 kHz. When approaching the sample surface, a decrease of the oscillation amplitude of the tuning fork is observed. The origin of this decrease is still not clearly understood. Several possible interaction mechanisms have been proposed as an explanation, e.g. capillary forces [2], van der Waals forces and actual contact between fiber and sample [8]. In this paper the effect of this interaction on the amplitude and phase of the oscillation of the tuning fork will be discussed and the consequences for the dynamics of a feedback mechanism acting on either one of these signals will be demonstrated. The results, however, are not limited to this specific tuning-fork shear-force system but can be more generally applied to all dynamic-mode distance regulation schemes, like tapping-mode and non-contact atomic force microscopy.

2. Implementation and detection system

The tuning fork is of a commercially available type and fabricated for "quartz" clocks. The resonance frequency is 32 768 Hz ($=2^{15}$ Hz). The spring constant of the tuning fork used in our experiments is 14.7 kN/m.

In operation, the tuning fork is externally vibrated by a driving peizoelement which is attached to the base of the tuning fork and is driving it near its resonance frequency. Both arms of the tuning fork move in the same direction. The amplitude of the tuning fork is detected by detecting the alternating signal from the tuning fork. A perfectly balanced tuning fork would not produce any current as both arms would move exactly identical. In our setup, however, the fiber is glued to one arm of the tuning fork leaving only a short part, 1 mm or less, unattached, and thereby changing the mass and stiffness of that arm. The resonance frequency of the short part of the fiber is kept higher than the resonance frequency of the tuning fork itself, because the oscillation of the tuning fork should be damped by the attached fiber interacting with the sample.

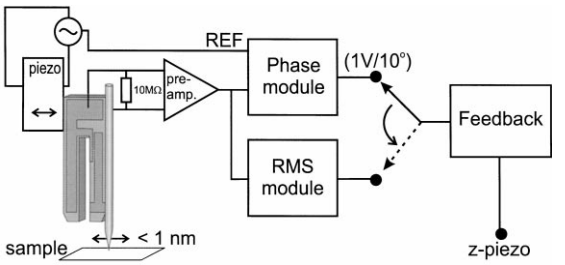

Fig. 1. Schematic of the detection system used to detect the piezoelectric tuning fork signal.

Fig. 1 displays the schematic of the tuning fork and the shear-force detection, as it has been implemented. The piezoelectric signal is detected over a 10 MΩ load resistor using a high-impedance instrumentation pre-amplifier (LT1105, 100×), and further amplified (10×) to achieve signal levels up to 10 V. From this signal the amplitude and phase are measured in two seperate modules. The measurement of the rms value of the amplitude is performed with a AD637 (RMS-to-DC converter), with a 5 kHz bandwidth. The phase difference between amplitude of the tuning fork and the driving voltage is measured in the phase module with a 2 kHz bandwidth and a gain of 1 V per 10° phase difference. The operation of the phase module is based on an XOR comparison between the reference signal and the amplitude of the tuning fork. This causes the phase signal to be linear with phase over a range of 180°, and inversely proportional to the phase the next 180°. The bandwidths of the modules are chosen to be larger than the first resonance frequency of the *xyz*-scanner, usually around 1 kHz.

3. Characterization and calibration

The characterization of the tuning fork system was performed using the scheme displayed in Fig. 2a.

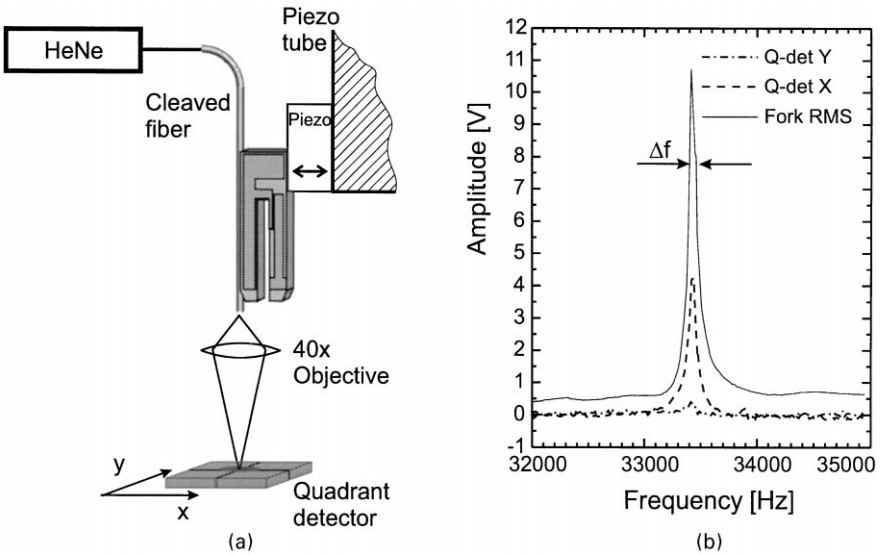

Fig. 2. (a) Schematic setup for the characterization of the tuning fork system, (b) resonance curve of the tuning fork with a fiber attached.

A single-mode fiber, cleaved at both ends, was glued to one arm of the tuning fork. The base of the tuning fork was attached to the driving piezolement (PXE 5, 0.5 nm/V, Philips), which in this case was mounted onto a piezotube used for *xyz*-scanning. The light from an HeNe-laser was coupled into the fiber and the output from the fiber was imaged onto a quadrant detector (SPOT-9D, Un. Det. Techn, CA) by a 40× objective (Nikon extra long working distance, 0.5 NA). The difference in photo-currents form the opposite halves of the detector is, for small oscillations, linearly related to the displacement of the fiber. To align the system, the objective was mounted on a three-axis translation stage, in order to create near-zero difference signals in the *x*- and *y*- direction of the quadrant detector. Final zeroing of the difference signals of the quadrant detector is performed electronically by adding/subtracting a manually adjustable voltage from the difference signals.

The resonance curve of the tuning fork and single-mode fiber was measured by sweeping the frequency of the driving piezoelement through the resonance frequency and simultaneously recording the output of the rms module and both difference signals of the quadrant detector. The results are displayed in Fig. 2b, where the frequency was varied between 32 and 35 kHz.

Upon attachment of the fiber the resonance frequency of the tuning fork system shifted from its original value of 32.768 kHz to approximately 33.400 kHz, while the *Q*-factor of the resonance, defined as $f_r/\Delta f$, dropped form $\sim 30\,000$ to approximately 1000. This indicates that the effect of stiffening, due to the addition of the fiber to the tuning fork, is larger than the effect of the increased mass of the tuning fork. The difference signals of the quadrant detector, represented by the dotted lines in Fig. 2b, verify was indeed moving along the *x*-direction in which the tuning fork was excited.

The difference signals of the quadrant detectors could be calibrated by displacing the tuning fork, using the piezotube scanner, for a known distance. Using this calibration an accurate determination of the tip amplitude versus the excitation voltage could be made. Fig. 3 displays the calibration curve, where the amplitude of the excitation voltage was varied between 1 mV and 20 V, and the root-mean-square value of the quadrant detector difference signal is measured at 5 kHz bandwidth, with a noise level of approximately 40 mV. For detected amplitudes exceeding this lower detection

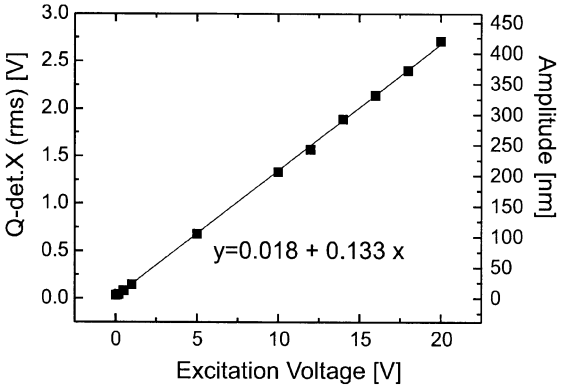

Fig. 3. Tip amplitude versus excitations amplitude. Left-axis: difference signal of the quadrant detector (V), right-axis: calibrated tip amplitude in nm.

limit, a linear behavior between excitation voltage and amplitude of the end of the fiber was found. If the assumption is made that this linear behavior extends for excitation amplitudes down in the mV ($\sim$ pm) range, an estimation can be made about the minimum detectable amplitude. The tuning fork signal (after $1000\times$ amplification) returned 3.5 V/nm (corresponding to 0.28 pm/mV) with a noise level of approximately 100 mV at 1 kHz bandwidth. This implies that the minimum detectable amplitude at this bandwidth is approximately 30 pm. With a spring constant of 14.7 kN/m the lateral force at this minimum amplitude at the end of the tuning fork is approximately 255 pN [4].

The derivative of the curve in Fig. 3 is 133 $mV_{rms}/V_{exc.}$, corresponding to 21 $nm/V_{exc.}$ With a Q-factor of 1000 the calibration factor of the driving piezo at 32 kHz is only 21 $pm/V_{exc,}$ which is more than one order of magnitude lower than the specification of 0.5 $nm/V_{exc.}$ Possible reasons for this could be a poor mechanical contact between driving piezo and tuning fork or a degrading of the piezoelectric material.

4. Approach experiment

In order to get a better understanding of the interaction mechanism a series of experiments have been performed. A tapered fiber probe was glued to one arm of a tuning fork (32 768 Hz) with its base attached to the driving piezoelement. The total system was mounted on an xyz scanner. The driving piezoelement was used to drive the tuning fork at frequencies between 32 630 and 32 740 Hz.

Measurements were performed detecting the rms and phase signal as a function of the driving frequency and probe-sample distance. Fig. 4 displays the rms signal and the phase signal as a function of driving frequency and tip–sample distance. The voltage on the driving piezoelement was 28 mV (peak–peak), and the quality factor of the fork out of contact was determined to be 1600. The sample consisted of freshly cleaved mica, in order to have a clean surface without a (water) contamination layer. The zero point on the z-displacement scale is chosen at an arbitrary position as the actual point of contact cannot be determined exactly.

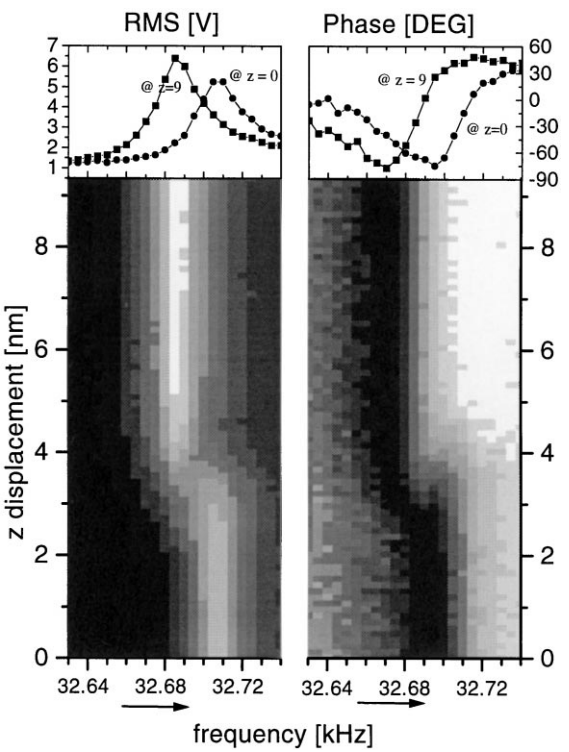

Fig. 4. Amplitude and phase as a function of driving frequency and tip–sample distance. TOP: cross-sections of amplitude and phase at $z = 0$ (in contact) and $z = 9$ (out of contact).

Approaching the sample, a change in the resonance frequency is observed. The resonance frequency shifted about 20 Hz to a higher frequency. Correspondingly, the 90° phase point shifted 20 Hz higher. The phase signal is only proportional with phase between 90° and −90° and inversely proportional with phase between −90° and −270° which caused the minimum in phase in Fig. 4 at −90°. The shift in resonance frequency of the tuning fork can be explained by its geometry. In contact, the amplitude at the endpoint of the fiber decreases, exerting a force on the tuning fork inversely proportional to the amplitude, thereby effectively enlarging the spring constant of the tuning fork. The Q-factor only slightly reduces compared to the out of contact value. Mainly a shift in resonance frequency is observed, which cannot be caused by a viscous damping of the oscillation, as this would cause a decrease in the resonance frequency ($\omega = \sqrt{k/m}\sqrt{1-\beta^2}$).

5. Numerical calculations

Exciting the tuning fork at constant frequency, one can apply feedback on either the rms signal or the phase signal. In practice, it is experienced that feedback on phase is faster than when using the rms signal. This can be explained by looking at the tuning fork as a second-order mechanical system [9]. The equation of motion is

$$\ddot{x} + 2\beta\omega_s\dot{x} + \omega_s^2 x = \frac{F_0}{m}\cos\omega_d t, \tag{1}$$

where x is the tuning fork deflection, m is the effective mass of the tuning fork, β is the damping constant, $\omega_s(=\sqrt{k/m})$ is the angular resonance frequency of the oscillating system, ω_d is the angular driving frequency and F_0 is the driving force. In contact the spring constant k increases, increasing ω_s, so that the system effectively gets driven off-resonance. Using $x(t) = \mathrm{Re}[\widehat{A}(t)\exp(\mathrm{i}\omega_d t)]$, it follows that

$$\ddot{\widehat{A}} + (2\mathrm{i}\omega_d + 2\beta\omega_s)\dot{\widehat{A}} + (\omega_s^2 - \omega_d^2 + 2\mathrm{i}\beta\omega_s\omega_d)\widehat{A} = F_0/m \tag{2}$$

with general solution

$$\widehat{A}(t) = \widehat{C}\exp(-\beta\omega_s t)\exp(\mathrm{i}(\omega_s\sqrt{1-\beta^2} - \omega_d)t) + \frac{F_0/m}{\omega_s^2 - \omega_d^2 + 2\mathrm{i}\beta\omega_s\omega_d}, \tag{3}$$

where $\widehat{C}$ is a complex constant to fit the boundary conditions. Applying a sudden frequency change from steady-state resonance at $t = 0$, $\widehat{C}$ is given by

$$\widehat{C} = \frac{F_0/m}{2\mathrm{i}\beta\omega_d^2} - \frac{F_0/m}{\omega_s^2 - \omega_d^2 + 2\mathrm{i}\beta\omega_s\omega_d}. \tag{4}$$

Analyzing $\widehat{A}(t)$ after the frequency change reveals that the phase, $\arg(\widehat{A}(t))$, has a maximum derivative directly after the frequency change, whereas the amplitude $|\widehat{A}(t)|$ does not instantaneously reach a maximum derivative, but shows a more continuous behavior.

To further illustrate this, a second-order tuning fork system has been numerically simulated using a driving frequency of $\omega_d/2\pi = 32\,000$ Hz, while the resonance frequency of the tuning fork system is varied with a modulation frequency (f_m), to simulate the tuning fork going in and out of contact with frequency f_m; thus $\omega_s/2\pi = 32\,005 + 5\sin(2\pi f_m t)$. The damping term and drive term are kept constant at $\beta\omega_s/2\pi = 16$ Hz (corresponding to $Q \approx 1000$) and $F_0/m = \omega_d^2\ \mathrm{ms}^{-2}$ for normalization.

Fig. 5 is obtained by calculating the amplitude and phase of the oscillation while modulating the resonance frequency with 10 Hz around 32 005 Hz at a modulation frequency of 40 Hz. During the first 20 ms the amplitude builds up towards the Q-value. It is observed that the relative signal change of the phase due to the modulation frequency ($\equiv$ modulation amplitude of the phase) is larger than that of the amplitude. It is further noted that the time lag between amplitude signal and $\sin(2\pi f_m t)$ is larger than the time lag between phase signal and $\sin(2\pi f_m t)$, indicating a larger modulation phase for the amplitude signal than for the phase signal. From Fig. 5 the modulation amplitude and the modulation phase of both signals can be determined at this modulation frequency of 40 Hz. By increasing the modulation frequency, the total frequency response of the rms and phase signals can be determined. The results are plotted in a gain-phase diagram, shown in Fig. 6.

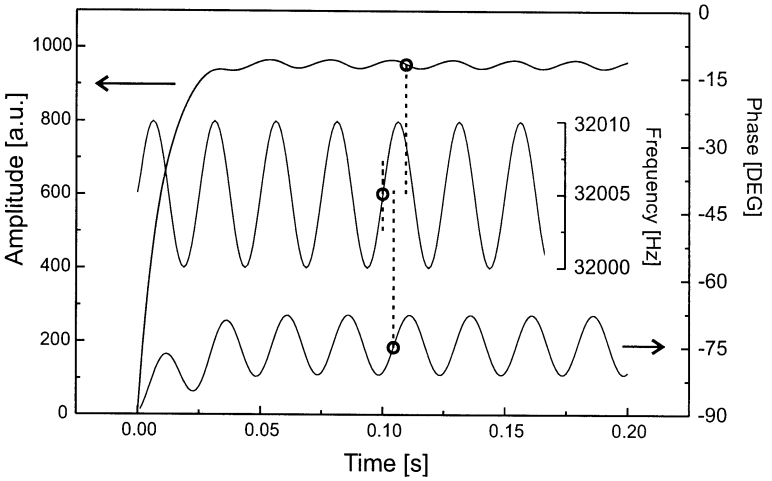

Fig. 5. Simulation of a second-order system, amplitude and phase as a function of time. At $t = 0$ the driver starts, the resonance frequency is $\omega_s(t)/2\pi = 32\,000 + 5 \times (1 + \sin(2\pi f_m t))$, modulated with $f_m = 40$ Hz. The inset displays $\omega_s(t)/2\pi$.

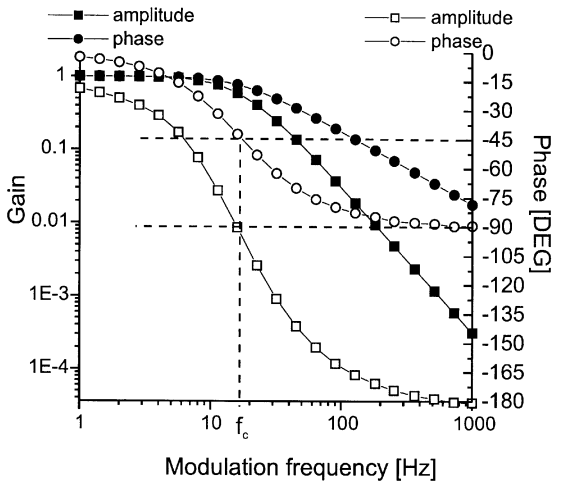

Fig. 6. Frequency response of both rms and phase signals as result of a series of simulations; normalized gain and modulation phase as function of the modulation frequency.

These results reveal that the rms-signal response curve corresponds to that of a second-order system, whereas the phase-signal response curve corresponds to that of only a first-order system. Both curves show the same cutoff frequency. From the exponential decay term of Eq. (3) this cutoff frequency can be derived:

$$f_c = \omega_{\text{cutoff}}/2\pi = \beta\frac{\omega_s}{2\pi} = \frac{\omega_s/2\pi}{2Q} \approx 16 \text{ Hz}. \quad (5)$$

So a cutoff frequency of 16 Hz is expected which agrees with Fig. 6. This has of course immediate consequences for the dynamics of a feedback system acting on either rms or phase signal. Especially, the modulation phase behavior of Fig. 6 limits the maximum frequency of the feedback system. Due to the limited bandwidth of our electronics and scanning system, and due to the control loop, an additional phase change will be added to the one displayed in Fig. 6, which causes a feedback system acting on the rms-signal to oscillate at a lower feedback bandwidth than a feedback system acting on the phase signal.

To verify this simulation experimentally, the dynamic behavior of the shear-force system has been investigated with a spectrum/network analyzer (HP 3589A). The output of the network analyzer generated a modulation of the z-displacement of the xyz-scanner (12 nm peak–peak) while rms and phase signals were monitored at the input. By doing so, the modulation gain and modulation phase of both signals could be determined. The initial tip–sample distance was less than 12 nm in order to

have the tip moving in and out of contact during one period of the modulation frequency.

The measurements are displayed in Fig. 7, and show good agreement with the simulated response. The gain of the rms signal drops with 12 dB/oct and the gain of the phase signal drops with exactly 6 dB/dot, indeed corresponding to a second- and first-order system, respectively. The modulation phase in Fig. 7 shows that the modulation phase of the rms signal changes twice as fast as the modulation phase of the tuning forks's phase signal. The changes, however, are not exactly 90° and 180° but are larger because of the additional phase change generated in the rest of our system, as mentioned previously. In Fig. 7 it can be seen that using rms signal, already at 80 Hz a change in modulation phase of 180° is reached, resulting in an unstable feedback system, whereas for the phase signal the change in modulation phase stays well within the 180° for the frequency range displayed. So although the cutoff frequency in the feedback circuit is located below 20 Hz the bandwidth of the feedback circuit can exceed this limit. It is primarily limited by the modulation phase behaviour displayed in Fig. 7 which stresses the benefit of a first-order response curve resulting in an increased feedback bandwidth.

6. Measurements on DNA

Experiments have been performed using the standalone version of shear-force microscope, in which the tuning fork, attached to a tube scanner, is scanned over the sample surface. In order to show that this system, based on phase signal feedback, can be used for imaging and that the forces between tip and sample necessary to induce this phase change are small double-stranded DNA was imaged. The DNA, dissolved in a $MgCl_2$ buffer, was precipitated on a mica surface [10]. The images shown in Fig. 8 were measured in the standalone

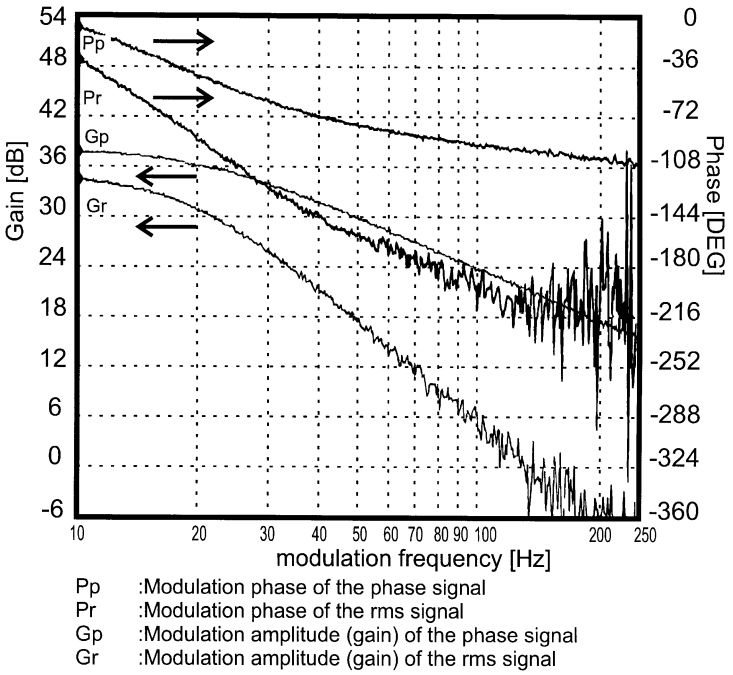

Fig. 7. Measurement of the (gain and phase) frequency response of both RMS and phase signals. The arrows denote the corresponding axis.

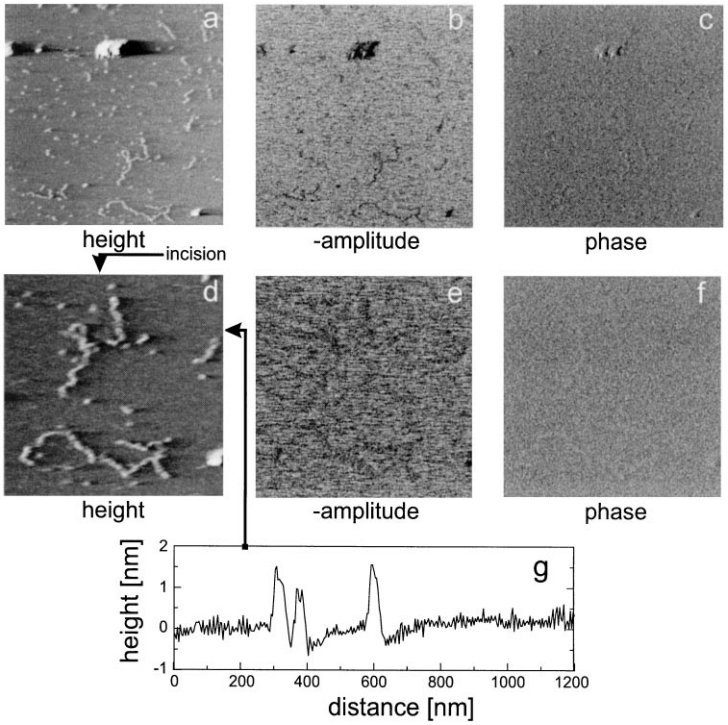

Fig. 8. Measurement of double-stranded DNA on mica, (a)–(c) image size 2.4×2.4 μm, (d)–(f) zoomed-in to an image size 1.2×1.2 μm, (g) line profile from (d) at the marked position.

shear-force microscope using phase feedback with a phase set-point close to the out of contact value. Images (a) and (b) display the *z*-signal from the *xyz*-scanner which is proportional to the height. Images (b) and (e) display the inverted amplitude of the tuning fork. When scanning over the DNA a slight increase in amplitude (darker in the image) is observed, indicating less interaction between the probe and the DNA as compared to the interaction between the probe and the mica. Images (c) and (f) display the phase signal which was used as feedback signal and therefore should be constant. The corresponding line trace, displayed in Fig. 8g, shows the height of the DNA as 1.4 ± 0.2 nm. Taking a few consecutive images no visible degradation of the DNA was noticed. However, by enlarging the phase set-point in the feedback system towards the in-contact value the DNA could be cut, as can be seen in image (d) by the vertical incision at a distance of 500 nm.

Based on the known structure of the double-stranded DNA, and measured with non-contact atomic force microscopy (AFM) [11], the height of the DNA is about 2 nm. The height of DNA measured by tapping-mode atomic force microscopy is usually a factor of 2 smaller than would be expected based on the known structure of double-stranded DNA. This effect is commonly attributed to indentation of the DNA [12–14]. The value measured with the shear-force microscope is 1.4 ± 0.2 nm which indicates a lower interaction with the DNA as compared to tapping-mode AFM.

Imaging the DNA with feedback on the rms signal using the same tip and setup resulted in a too unstable feedback to generate an image of comparable quality. After vibration reduction, by suspending the setup to the ceiling by elastic cords, feedback on amplitude was possible, however, only with reduced feedback bandwidth.

7. Conclusions

It can be concluded that by using feedback on the phase of the oscillation of the tuning fork an increased bandwidth in the feedback system can be applied as compared to feedback on the rms signal resulting in higher applicable scan speeds. The experiments on DNA show that using the shear-force microscope, a more realistic height of the DNA is measured as compared to regular tapping-mode AFM.

Acknowledgements

S.J.T. van Noort is acknowledged for preparing the DNA sample. This work was mainly supported by the Dutch organization for fundamental research on matter (FOM).

References

[1] E. Betzig, P.L. Finn, J.S. Weiner, Appl. Phys. Lett. 60 (1992) 2484.
[2] R. Toledo-Crow, P.C. Yang, Y. Chen, M. Vaez-Iravani, Appl. Phys. Lett. 60 (1992) 2957.
[3] Bert Hecht, Thesis, Swiss Federal Inst. of Techn., ETH Zurich, Swiss, 1996.
[4] K. Karrai, R.D. Grober, Appl. Phys. Lett. 66 (1995) 1842.
[5] J.W.P. Hsu, M. Lee, B.S. Deaver, Rev. Sci. Instr. 66 (1995) 3177.
[6] J. Barenz, O. Hollricher, O. Marti, Rev. Sci. Instr. 67 (1996) 1912.
[7] M. Lee, B. McDaniel, J.W.P. Hsu, Rev. Sci. Instr. 67 (1996) 1468.
[8] M.J. Gregor, P.G. Blome, J. Schöfer, R.G. Ulbrich, Appl. Phys. Lett. 68 (1996) 307.
[9] T.R. Albrecht, P. Grütter, D. Horne, D. Rugar, J. Appl. Phys. 69 (1991) 668.
[10] J.P. Vesenka, M. Guthold, C. Tang, D. Keller, E. Delaine, C.J. Bustamante, Ultramicroscopy 42–44 (1992) 1243.
[11] D. Anselmetti, M. Dreier, R. Lüthi, T. Richmond, E. Meyer, J. Frommer, H.-J. Günterodt, J. Vac. Sci. Technol. B 12 (3) (1994) 1500.
[12] C.E. Wyman, E. Grotkopp, C. Bustamante, H.C.M. Nelson, EMBO J. 14 (1995) 117.
[13] G. Yang, J.P. Vesenka, C.J. Bustamante, Scanning 18 (1955) 344.
[14] S.J.T. van Noort, K.O. van Werf, B.G. de Grooth, N.F. van Hulst, J. Greve, Ultramicroscopy, 69 (1997) 117.